

# Nanostructure for near total light absorption in a monolayer of graphene in the visible

AMIRREZA MAHIGIR<sup>1,2</sup>  AND GEORGIOS VERONIS<sup>1,2,\*</sup>

<sup>1</sup>School of Electrical Engineering and Computer Science, Louisiana State University, Baton Rouge, Louisiana 70803, USA

<sup>2</sup>Center for Computation and Technology, Louisiana State University, Baton Rouge, Louisiana 70803, USA

\*Corresponding author: gveronis@lsu.edu

Received 27 August 2018; revised 31 October 2018; accepted 4 November 2018; posted 5 November 2018 (Doc. ID 344261); published 30 November 2018

**We propose a highly compact structure for near total light absorption in a monolayer of graphene in the visible. The structure consists of a grating slab covered with the graphene monolayer. The grating slab is separated from a metallic back reflector by a dielectric spacer. The structure supports a guided resonance in the visible. We show that such a structure enhances light–matter interactions in graphene via critical coupling by matching the external leakage rate of the guided resonance and the intrinsic loss rate in the system. We also show that, by using the dielectric spacer between the grating and the metallic mirror, near total absorption in the graphene monolayer can be achieved in the visible without the need for thick multilayer dielectric mirrors. The proposed structure could find applications in the design of efficient nanoscale visible-light photodetectors and modulators.** ©2018 Optical Society of America

<https://doi.org/10.1364/JOSAB.35.003153>

## 1. INTRODUCTION

During the past few years, graphene has been the subject of a great amount of research for developing optoelectronic and photonic devices, owing to its unique electronic and optical properties [1–13]. However, the absorption rate in graphene is limited due to its ultra-thin monolayer structure. A suspended pure graphene monolayer (~0.34 nm thickness) exhibits absorption of ~2.3% in the near-infrared to visible spectral range [7]. This weak absorption limits the efficiency of graphene-based devices. Although absorption enhancement in graphene in the near infrared has been extensively investigated in recent years [14–20], increasing light absorption in graphene in the visible is still a challenge due to parasitic absorption from other materials at visible wavelengths. As an example, the use of metallic reflectors results in significant suppression of absorption in graphene in the visible, due to parasitic losses in the metal. Even though losses could be greatly reduced by using multilayer dielectric Bragg mirrors instead of metallic mirrors, the use of dielectric Bragg mirrors not only greatly adds to the physical footprint of the device, it also makes the fabrication process more complicated since it requires material deposition of several layers [21,22].

Recently, total absorption in a graphene monolayer in the optical regime using the concepts of critical coupling and guided resonance was reported [22]. It was demonstrated that a photonic crystal structure backed by a mirror greatly enhances light–matter interactions in the graphene monolayer. In some

related recent studies, enhanced absorption in a graphene monolayer was reported in structures with metallic reflectors in which graphene was placed on top of a dielectric slab, while a dielectric grating structure was deposited on the top surface of the graphene layer [20,23–25]. In such a structure, with proper choice of dimensions and materials, one can enhance light–graphene interactions by exploiting critical coupling between the graphene monolayer and a guided resonance mode of the grating. The fabrication of such structures is challenging since deposition of materials on top of the graphene layer is required. In addition, this process can degrade the quality of graphene [26] and makes the addition of contact electrodes to graphene complicated.

In this paper, we propose a grating slab structure covered by a graphene monolayer that supports a guided resonance at visible wavelengths and enhances light–matter interactions in graphene via critical coupling. We use a metallic back reflector that makes the proposed structure very compact with an overall thickness of less than one wavelength. In addition, the grating slab is separated from the metallic back reflector by a dielectric spacer. We show that, by using the dielectric spacer between the grating and the metallic mirror, near total absorption in the graphene monolayer can be achieved in the visible without the need for thick multilayer dielectric mirrors. In addition, in our proposed structure no deposition on top of graphene is required, resulting in a simple fabrication process, in which the quality of graphene is not compromised. We find that in

the proposed structure the absorption in the graphene monolayer is enhanced to  $\sim 100\%$  at visible wavelengths, making this structure suitable for the design of efficient nanoscale visible-light photodetectors and modulators.

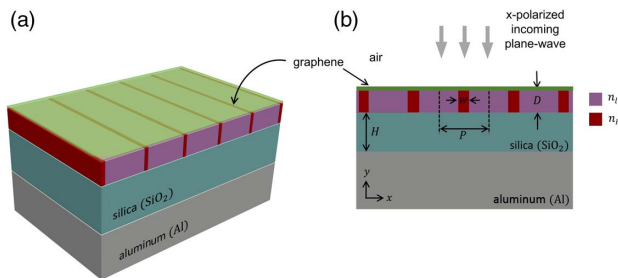
## 2. DESIGN AND THEORY

Figure 1(a) shows the schematic of the proposed structure. A graphene monolayer is placed on top of a grating slab, which is separated from a metallic back reflector by a dielectric spacer. The grating slab consists of high-index and low-index dielectric rods with refractive indices  $n_h$  and  $n_l$ , respectively, which are periodically repeated. An appropriate choice of the periodicity of the grating slab results in phase-matched coupling between the guided mode of the slab and free space fields, forming a guided resonance. We choose the grating slab materials and physical dimensions to create a guided resonance at visible wavelengths in the slab.

Dielectric Bragg mirrors are preferred over metallic back reflectors, because the proximity of metals to the resonant fields leads to parasitic absorption in the metal, resulting in suppression of the absorption in graphene [22]. However, since dielectric Bragg mirrors require at least five to seven pairs of alternating dielectric layers for maximum reflection, they greatly add to the overall thickness of the structure [21,22]. In addition, the fabrication of dielectric Bragg mirrors is relatively more complicated, since it requires deposition of multiple layers. On the other hand, using metallic reflectors results in more compact structures with a simpler fabrication process. Here, we therefore choose an aluminum (Al) back reflector separated from the grating slab by a dielectric spacer, which prevents the formation of strong surface plasmon resonances on the surface of the metal. This design approach enables us to almost eliminate parasitic absorption in the metal, leading to near total light absorption in graphene at visible wavelengths. We found that, since in our structure we minimize the coupling of the guided resonance fields with the metallic back reflector, the choice of metal does not significantly affect the results.

### A. Design of the Structure

We design the grating slab to support only the zeroth order diffraction outside the slab at the wavelength of interest ( $\lambda_0 = 600$  nm), to prevent any optical loss through higher



**Fig. 1.** (a) Schematic of a structure for enhancing light absorption in a monolayer of graphene (shown as a transparent green layer at the top of the structure) using a grating slab, a dielectric spacer (silica), and a metallic back reflector (aluminum). (b) Cross-sectional view of the structure shown in (a). Incoming light polarization is along the  $x$  direction. The light is normally incident from above.

order diffracted waves, and only the first order diffraction inside the slab, giving rise to the first guided resonance of the slab (Fig. 2). By matching the external leakage rate of this guided resonance with the intrinsic loss rate in the system, we satisfy the critical coupling condition, resulting in enhanced absorption in graphene. We start with the grating diffraction equation for the reflected waves [27],

$$n_r \sin \theta_m^r = n_{\text{inc}} \sin \theta_{\text{inc}} + m \frac{\lambda_0}{P}, \quad (1)$$

where  $n_r$  and  $n_{\text{inc}}$  are the refractive indices of the materials in which the diffracted and incident waves propagate, respectively (Fig. 2). In addition,  $m$  is the diffraction order, while  $\theta_{\text{inc}}$  and  $\theta_m^r$  are the angles corresponding to the incident and diffracted waves, respectively. Finally,  $P$  and  $\lambda_0$  are the period of the structure and the wavelength of interest, respectively. Here, we choose  $\lambda_0 = 600$  nm. The material above the structure is air, so that  $n_r = n_{\text{inc}} = 1$ . Since the incoming wave is normally incident on the grating slab, we have  $\theta_{\text{inc}} = 0$ . This simplifies Eq. (1) to

$$\sin \theta_m^r = m \frac{\lambda_0}{P}. \quad (2)$$

To eliminate any diffraction order higher than the zeroth order ( $m = 0$ ) outside the slab, we choose the periodicity  $P = 300$  nm, which is smaller than the wavelength of interest  $\lambda_0$ . Then, for any  $m \neq 0$  we have  $|m \frac{\lambda_0}{P}| > 1$ , so that all higher diffraction orders are eliminated [Eq. (2)]. By tuning the thickness of the dielectric spacer  $H$  [Fig. 1(b)], the zeroth order diffraction will also be eliminated, resulting in near total light coupling to the guided resonance of the grating slab. For the transmitted waves, the grating diffraction equation becomes

$$n_t \sin \theta_m^t = n_{\text{inc}} \sin \theta_{\text{inc}} + m \frac{\lambda_0}{P}. \quad (3)$$

Here  $\theta_m^t$  is the angle of the  $m$ th transmitted wave, and  $n_t$  is the effective refractive index of the grating slab, satisfying the following equation [28]:

$$n_t^2 = \frac{n_h^2 n_l^2}{f n_l^2 + (1-f) n_h^2}, \quad (4)$$

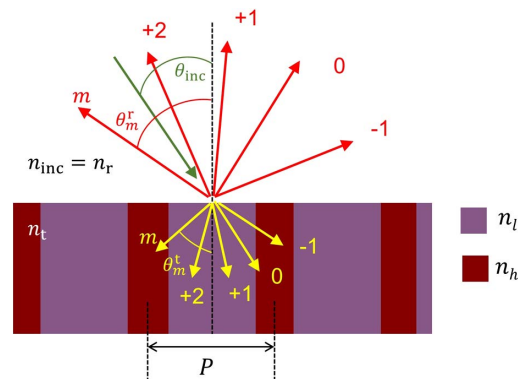


**Fig. 2.** Diffracted waves in the grating slab. Here,  $\theta_{\text{inc}}$ ,  $\theta_m^r$ , and  $\theta_m^t$  are the angles of the incident wave, of the  $m$ th reflected wave, and of the  $m$ th transmitted wave, respectively.

where  $f = \frac{w}{p}$  is the fill factor. The effective refractive index  $n_t$  should be tuned in such a way that only the first diffraction order exists in the slab, and higher diffraction orders are evanescent. Imposing these criteria to Eq. (3), we obtain

$$|\sin \theta_1^t| = \frac{\lambda_0}{n_t P} < 1, \quad (5)$$

and

$$|\sin \theta_2^t| = 2 \frac{\lambda_0}{n_t P} > 1. \quad (6)$$

Substituting  $P = 300$  nm and  $\lambda_0 = 600$  nm in Eqs. (5) and (6) above, we obtain  $2 < n_t < 4$ . This is the range for the effective refractive index  $n_t$ , allowing the formation of the first diffraction order in the slab and also eliminating all higher diffraction orders. If we choose  $n_t$  to be in this range by tuning the fill factor  $f$ , we can match the leakage rate of the guided resonance out of the slab to the intrinsic loss rate in the system, so as to satisfy the critical coupling condition, and enhance the absorption in graphene to  $\sim 100\%$ .

It should be noted that the existence of a guided resonance is due to total internal reflection from the boundaries between the grating slab and the surrounding materials. We therefore choose silica ( $\text{SiO}_2$ ) for the dielectric spacer with refractive index  $n_{\text{SiO}_2} \sim 1.4$ , which is smaller than  $n_t$ . We also choose the thickness of the grating slab to be  $D = 150$  nm, which is much smaller than the operating wavelength of 600 nm, to keep the resonator modes to zeroth order in the transverse direction [22].

## B. Critical Coupling Condition

We account for the numerical simulation results for the structure of Fig. 1 using coupled mode theory. The guided mode in the grating slab is a resonance with stored energy  $|a|^2$  at the resonance frequency  $\omega_0$ , interacting with input and output waves of amplitude  $u$  and  $y$ , respectively, with power given by  $|u|^2$  and  $|y|^2$ . If the time rate of amplitude change for the guided resonance in the grating slab without any input wave is given by the external leakage rate  $\gamma_e$ , then, using energy conservation and time reversibility arguments, it can be shown that the energy transfer rates between the incoming wave and the cavity and between the outgoing wave and the cavity are both proportional to  $2\gamma_e$  [22,29]. Considering a material loss rate  $\sigma$ , which includes both graphene and metal losses, the system can be described by the following equations [22]:

$$\dot{a} = (j\omega - \gamma_e - \sigma)a + \sqrt{(2\gamma_e)u}, \quad (7)$$

$$y = \sqrt{2\gamma_e}a - u. \quad (8)$$

Using these, we obtain the reflection coefficient

$$\Gamma = \frac{y}{u} = \frac{j(\omega - \omega_0) + \sigma - \gamma_e}{j(\omega - \omega_0) + \sigma + \gamma_e}, \quad (9)$$

and the absorption

$$A = 1 - |\Gamma|^2 = \frac{4\sigma\gamma_e}{(\omega - \omega_0)^2 + (\sigma + \gamma_e)^2}. \quad (10)$$

Equation (10) shows that, if the external leakage rate is equal to the intrinsic loss rate in the structure ( $\gamma_e = \sigma$ ), the critical

coupling condition is satisfied, and all of the incident light power is absorbed on resonance ( $\omega = \omega_0$ ). In the grating slab structure of Fig. 1, the external leakage rate of the guided resonance in the slab can be controlled by the fill factor  $f = \frac{w}{p}$ . Thus, by tuning the width  $w$  of the high-index dielectric rod in the slab, it is possible to achieve critical coupling.

## 3. RESULTS

We use full-wave finite-difference time-domain (FDTD) simulations (Lumerical FDTD Solutions). Graphene is modeled as a two-dimensional (2D) material based on its surface conductivity [30]. The surface conductivity is tuned to give 2.3% light absorption in a single graphene layer suspended in air in the visible and near-infrared wavelength ranges [7]. We use a plane wave with electric field polarization along the  $x$  direction to excite the structure [Fig. 1(b)]. Periodic boundary conditions and perfectly matched layer (PML) boundary conditions are used in the  $x$  and  $y$  directions, respectively. The absorption in the monolayer of graphene is given by [18,30,31]

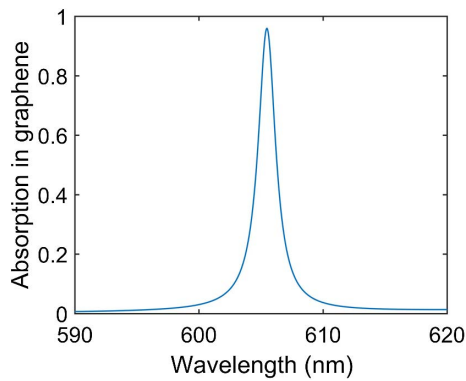
$$P_{\text{abs}}(\omega) = \frac{1}{2} \int_P \sigma_{gr}(\omega) |E(\omega)|^2 dl, \quad (11)$$

where  $\sigma_{gr}(\omega)$  is the surface conductivity of graphene, and  $|E(\omega)|^2$  is the intensity of the local electric field on the surface of graphene.

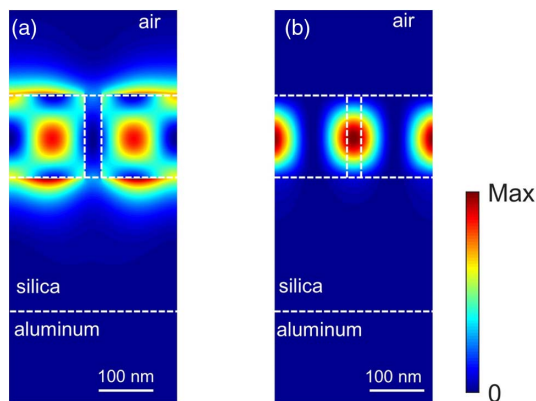
We choose gallium phosphide (GaP) ( $n \sim 3.3$ ) and titanium dioxide ( $\text{TiO}_2$ ) ( $n \sim 2.6$ ) as the high-index and low-index dielectric materials, respectively, in the grating slab. We use experimental data for the refractive indices of GaP,  $\text{TiO}_2$ , and Al [32–34]. Although silicon (Si) ( $n \sim 3.3$ – $3.4$ ) has almost the same refractive index as GaP, the band gap of silicon is  $\sim 1.1$  eV, which makes silicon opaque at visible wavelengths. On the other hand, GaP has a band gap of  $\sim 2.26$  eV, which makes it transparent at wavelengths longer than  $\sim 548$  nm.  $\text{TiO}_2$  is a lossless dielectric in the entire visible range. The widths of the high-index and low-index dielectric rods are chosen to be 30 nm and 270 nm, respectively, in one period of the grating slab [Fig. 1(b)]. In other words, the fill factor is  $f = \frac{w}{p} = 0.1$ , and from Eq. (4) we obtain  $n_t \sim 2.67$ .

Figure 3 shows the numerically calculated absorption spectra in the graphene monolayer for the structure of Fig. 1, optimized for maximum absorption around the operating wavelength of 600 nm. The spectra of Fig. 3 show near total ( $\sim 95\%$ ) absorption in the graphene monolayer at the wavelength of 605 nm. Thus, we achieve near total absorption in an atomically thin layer of graphene in the visible wavelength range. In addition, the width of the resonance is very narrow with less than  $\sim 2$  nm full width at half-maximum. This is an attractive feature of the structure for applications related to photodetectors and modulators. About 5% of the incident light power is absorbed in the metallic back reflector.

The electric and magnetic field amplitude profiles of the guided resonance in the resonator are shown in Fig. 4(a) and 4(b), respectively. As these profiles reveal, the fields are mostly confined in the grating slab region, thus minimizing the parasitic losses in the metal. The proposed structure can therefore be used as a high-performance and compact system



**Fig. 3.** Calculated absorption spectra in the graphene monolayer for the structure shown in Fig. 1 for normally incident light. GaP and TiO<sub>2</sub> are used as the high-index ( $n_h \sim 3.3$ ) and low-index ( $n_l \sim 2.6$ ) materials, respectively, in the grating slab. The widths of the high-index and low-index dielectric rods in the slab are 30 nm and 270 nm, respectively. The period of the structure  $P$ , the slab thickness  $D$ , and the silica spacer thickness  $H$  are 300 nm, 150 nm, and 300 nm, respectively. Near total absorption occurs in the visible ( $\lambda_0 \approx 605$  nm).



**Fig. 4.** (a) Electric and (b) magnetic field amplitude profiles for the structure of Fig. 1 at the wavelength of 605 nm. The boundaries of the grating slab, silica spacer, and metallic back reflector are indicated with dashed white lines. All other parameters are as in Fig. 3.

to efficiently enhance light–matter interactions in the graphene monolayer at visible wavelengths.

Figure 5 shows the reflection from the structure as a function of the silica spacer thickness  $H$ , when the incoming free space plane wave is normally incident from above. Owing to Fabry–Perot effects in the silica spacer, its thickness  $H$  greatly influences the reflection from the structure. In the optimized structure we choose the silica thickness to be  $H = 300$  nm. For this thickness the reflection from the structure vanishes, and all of the incident power is absorbed. We also found that varying the silica spacer thickness has no significant effect on the resonance wavelength of the guided mode. The effect of the thickness of the silica spacer can also be understood using the concept of the effective impedance of the structure [35]. When the silica spacer thickness is  $H = 300$  nm, the effective impedance of the structure matches the impedance of free space,

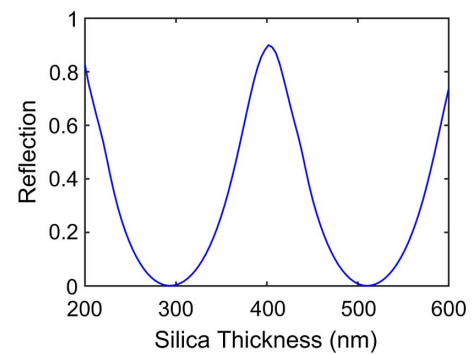


**Fig. 5.** Reflection from the structure of Fig. 1 for normally incident light as a function of the silica spacer thickness  $H$ . All other parameters are as in Fig. 4. For silica thickness of  $H = 300$  nm, the effective impedance of the structure almost matches the one of free space, resulting in close to zero reflection, and near perfect coupling of free space incident light to the guided resonance of the grating slab.

resulting in the elimination of the zeroth diffraction order, and near perfect light coupling to the guided resonance of the grating slab at the wavelength of 605 nm. It should be noted that, for silica thicknesses  $H$  below 200 nm, because of the proximity of the metallic surface to the strong guided resonance fields of the grating slab, parasitic surface plasmon resonances at the metal–silica interface greatly suppress absorption in graphene. As a result, the smallest silica spacer thickness for which reflection vanishes and near total absorption in graphene occurs in the structure is  $H = 300$  nm.

In Fig. 6 we compare the overall absorption spectra of the structure of Fig. 1 calculated using full-wave FDTD simulations to the spectra obtained using coupled-mode theory. To obtain the coupled-mode theory results, we perform FDTD simulations with the graphene monolayer removed and aluminum replaced with a perfect electric conductor, and we save the electric field as a function of time at multiple locations in the grating slab. For this lossless structure, we then calculate the Fourier transform of the average electric field at these locations, and fit the spectrum with a Lorentzian function,

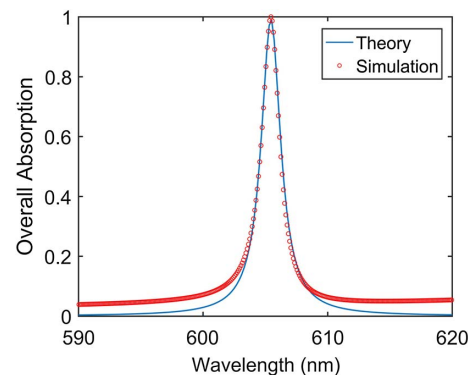


**Fig. 6.** Overall absorption spectra of the structure of Fig. 1 for normally incident light, calculated using full-wave FDTD simulations (red circles), and coupled-mode theory (solid line). All parameters are as in Fig. 3. The theory is in excellent agreement with the simulations in the vicinity of the resonance peak.

corresponding to the guided resonance of the grating slab. The center frequency of the Lorentzian gives the resonance frequency  $\omega_0$ , and the half-width at half-maximum gives the external leakage rate  $\gamma_e$  [22]. When we repeat the calculation for the lossy system, including the graphene monolayer and the aluminum back reflector, the half-width at half-maximum gives us  $\sigma + \gamma_e$ , and we can therefore obtain the intrinsic loss rate  $\sigma$  of the structure. We finally substitute the calculated parameters in Eq. (10) and obtain the coupled-mode theory results shown in Fig. 6. We observe that in the vicinity of the resonance the coupled-mode theory results are in perfect agreement with the full-wave FDTD simulation results. Away from the resonance, the coupled-mode theory results deviate from the simulation results, since the coupled-mode theory does not account for the losses of the system at off-resonance wavelengths [22].

In Fig. 7, we investigate the effect of the grating slab thickness  $D$  on the absorption spectra of the structure of Fig. 1. If the thickness of the slab is decreased, the guided resonance shifts to shorter wavelengths. Similarly, increasing  $D$  pushes the resonance to longer wavelengths. Thus, after achieving the critical coupling condition, one can adjust the resonance wavelength of the structure by tuning the grating slab thickness  $D$ , while maintaining near total absorption in the graphene monolayer. However, it should be noted that GaP becomes opaque for wavelengths shorter than  $\sim 548$  nm. Therefore, one cannot decrease the grating slab thickness  $D$  to achieve near total absorption in the graphene monolayer at arbitrarily short wavelengths.

Finally, in Fig. 8 we show the absorption spectra as a function of wavelength and angle of incidence for the structure of Fig. 1. The magnetic field of the incident wave is along the  $z$  direction. We observe that there is a broad angular range where strong absorption occurs. We also observe that the resonance exhibits frequency splitting and a substantial shift as the angle of incidence is varied.

We note that the absorption spectra of our proposed structure exhibit anisotropy with respect to the polarization of the incident light, similar to graphene nanoribbon structures

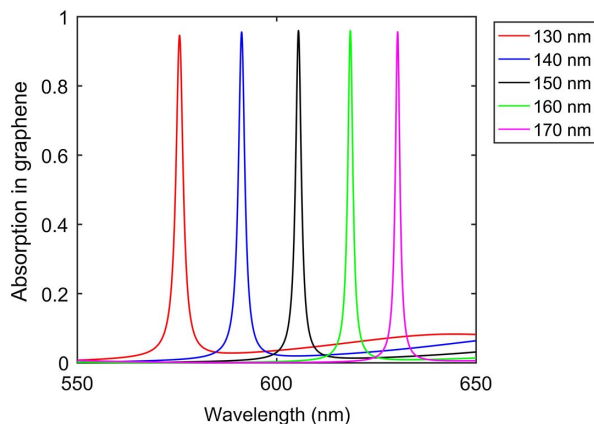


**Fig. 7.** Calculated absorption spectra in the graphene monolayer for the structure shown in Fig. 1 for normally incident light. Results are shown for different grating slab thicknesses  $D$ . All other parameters are as in Fig. 3. The absorption peak can be tuned over a wide wavelength range.

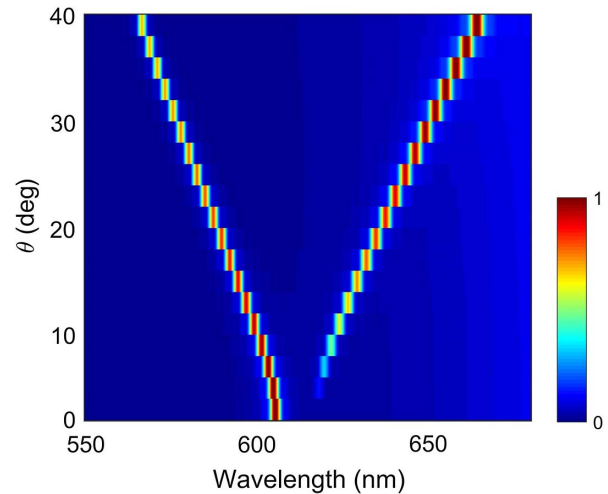


**Fig. 8.** Absorption spectra as a function of wavelength and angle of incidence for the structure of Fig. 1. The magnetic field of the incident wave is along the  $z$  direction. All other parameters are as in Fig. 3.

[36–39]. In other words, the absorption spectra for light with the electric field along the  $x$  direction are different from the absorption spectra for light with the electric field along the  $z$  direction. We also note that here the proposed nanostructure was optimized for electric field polarization along the  $x$  direction (Fig. 1). We found that for electric field polarization along the  $z$  direction the absorption spectra also exhibit peaks in the visible wavelength range. However, to achieve near total light absorption in the monolayer of graphene for electric field polarization along the  $z$  direction the proposed nanostructure would have to be optimized for this polarization to achieve the critical coupling condition.

## 4. CONCLUSIONS

In this paper, we achieved near total light absorption in a graphene monolayer in the visible wavelength range through enhancing light–matter interactions between the fields of the guided resonance of a grating slab and the graphene monolayer. We showed that an appropriate design of the structure enables critical coupling between the guided resonance and the graphene monolayer, resulting in intensified absorption in graphene. We also showed that using an appropriate dielectric spacer minimizes coupling of the guided resonance fields with the metallic back reflector, preventing any absorption suppression in graphene due to parasitic losses in the metal.

In our design, the graphene monolayer is placed on top of a grating slab and is not covered by other structures, so that the quality of graphene remains high and the fabrication process is relatively simple. While in this paper we designed the structure for graphene, the same design approach can be applied to achieve near total absorption in the visible in other atomically thin materials. The proposed structure could find applications in the design of nanoscale optoelectronic devices.

**Funding.** National Science Foundation (NSF) (1254934).

**Acknowledgment.** Portions of this work were presented at the CLEO conference in 2018, paper JTh2A.55.

## REFERENCES

1. F. J. Garcia de Abajo, "Graphene nanophotonics," *Science* **339**, 917–918 (2013).
2. A. Vakil and N. Engheta, "Transformation optics using graphene," *Science* **332**, 1291–1294 (2011).
3. F. Bonaccorso, Z. Sun, T. Hasan, and A. C. Ferrari, "Graphene photonics and optoelectronics," *Nat. Photonics* **4**, 611–622 (2010).
4. F. H. L. Koppens, T. Mueller, P. Avouris, A. C. Ferrari, M. S. Vitiello, and M. Polini, "Photodetectors based on graphene, other two-dimensional materials and hybrid systems," *Nat. Nanotechnol.* **9**, 780–793 (2014).
5. J. T. Liu, N. H. Liu, J. Li, X. J. Li, and J. H. Huang, "Enhanced absorption of graphene with one-dimensional photonic crystal," *Appl. Phys. Lett.* **101**, 052104 (2012).
6. M. Liu, X. Yin, E. Ulin-Avila, B. Geng, T. Zentgraf, L. Ju, F. Wang, and X. Zhang, "A graphene-based broadband optical modulator," *Nature* **474**, 64–67 (2011).
7. R. R. Nair, P. Blake, A. N. Grigorenko, K. S. Novoselov, T. J. Booth, T. Stauber, N. M. Peres, and A. K. Geim, "Fine structure constant defines visual transparency of graphene," *Science* **320**, 1308 (2008).
8. M. Bernardi, M. Palumbo, and J. C. Grossman, "Extraordinary sunlight absorption and one nanometer thick photovoltaics using two-dimensional monolayer materials," *Nano Lett.* **13**, 3664–3670 (2013).
9. S. C. Song, Q. Chen, L. Jin, and F. H. Sun, "Great light absorption enhancement in a graphene photodetector integrated with a metamaterial perfect absorber," *Nanoscale* **5**, 9615–9619 (2013).
10. W. S. Zhao, K. F. Shi, and Z. L. Lu, "Greatly enhanced ultrabroadband light absorption by monolayer graphene," *Opt. Lett.* **38**, 4342–4345 (2013).
11. X. Zhu, L. Shi, M. Schmidt, A. Boisen, O. Hansen, J. Zi, S. Xiao, and N. Mortensen, "Enhanced light-matter interactions in graphene-covered gold nanovoid arrays," *Nano Lett.* **13**, 4690–4696 (2013).
12. P. Avouris and M. Freitag, "Graphene photonics, plasmonics, and optoelectronics," *IEEE J. Sel. Top. Quantum Electron.* **20**, 72–83 (2014).
13. M. Hashemi, M. H. Farzad, N. A. Mortensen, and S. S. Xiao, "Enhanced absorption of graphene in the visible region by use of plasmonic nanostructures," *J. Opt.* **15**, 055003 (2013).
14. J. Hu, Y. Qing, S. Yang, Y. Ren, X. Wu, W. Gao, and C. Wu, "Tailoring total absorption in a graphene monolayer covered subwavelength multilayer dielectric grating structure at near-infrared frequencies," *J. Opt. Soc. Am. B* **34**, 861–868 (2017).
15. L. Zhang, L. L. Tang, W. Wei, X. L. Cheng, W. Wang, and H. Zhang, "Enhanced near-infrared absorption in graphene with multilayer metal-dielectric-metal nanostructure," *Opt. Express* **24**, 20002–20009 (2016).
16. J. P. Wu, L. Y. Jiang, J. Guo, X. Y. Dai, Y. J. Xiang, and S. C. Wen, "Tunable perfect absorption at infrared frequencies by a graphene-hBN hyper crystal," *Opt. Express* **24**, 17103–17114 (2016).
17. C. C. Guo, Z. H. Zhu, X. D. Yuan, W. M. Ye, K. Liu, J. F. Zhang, W. Xu, and S. Q. Qin, "Experimental demonstration of total absorption over 99% in the near infrared for monolayer-graphene-based subwavelength structures," *Adv. Opt. Mater.* **4**, 1955–1960 (2016).
18. B. Zhao, J. M. Zhao, and Z. M. Zhang, "Resonance enhanced absorption in a graphene monolayer using deep metal gratings," *J. Opt. Soc. Am. B* **32**, 1176–1185 (2015).
19. F. Xiong, J. F. Zhang, Z. H. Zhu, X. D. Yuan, and S. Q. Qin, "Ultrabroadband, more than one order absorption enhancement in graphene with plasmonic light trapping," *Sci. Rep.* **5**, 16998 (2015).
20. M. Grande, M. A. Vincenti, T. Stomeo, G. V. Bianco, D. de Ceglia, N. Akozbek, V. Petruzzelli, G. Bruno, M. De Vittorio, M. Scalora, and A. D'Orazio, "Graphene-based perfect optical absorbers harnessing guided mode resonances," *Opt. Express* **23**, 21032–21042 (2015).
21. J. R. Tischler, M. S. Bradley, and V. Bulović, "Critically coupled resonators in vertical geometry using a planar mirror and a 5 nm thick absorbing film," *Opt. Lett.* **31**, 2045–2047 (2006).
22. J. R. Piper and S. H. Fan, "Total absorption in a graphene mono layer in the optical regime by critical coupling with a photonic crystal guided resonance," *ACS Photon.* **1**, 347–353 (2014).
23. G. G. Zheng, X. J. Zou, Y. Y. Chen, L. H. Xu, and Y. Z. Liu, "Tunable spectrum selective enhanced absorption of monolayer graphene in Fano resonant waveguide grating with four-part period," *Plasmonics* **12**, 1177–1181 (2017).
24. R. Wang, T. Sang, L. Wang, J. Gao, Y. K. Wang, and J. C. Wang, "Enhanced absorption of a monolayer graphene using encapsulated cascaded gratings," *Optik* **157**, 651–657 (2018).
25. Y. S. Fan, C. C. Guo, Z. H. Zhu, W. Xu, F. Wu, X. D. Yuan, and S. Q. Qin, "Monolayer-graphene-based perfect absorption structures in the near infrared," *Opt. Express* **25**, 13079–13086 (2017).
26. K. S. Kim, Y. Zhao, H. Jang, S. Y. Lee, J. M. Kim, K. S. Kim, J. H. Ahn, P. Kim, J. Y. Choi, and B. H. Hong, "Large-scale pattern growth of graphene films for stretchable transparent electrodes," *Nature* **457**, 706–710 (2009).
27. E. G. Loewen and E. Popov, *Diffraction Gratings and Applications* (CRC Press, 1997).
28. D. E. Aspnes, "Bounds on allowed values of the effective dielectric function of two-component composites at finite frequencies," *Phys. Rev. B* **25**, 1358–1361 (1982).
29. W. Suh and S. H. Fan, "All-pass transmission or flat-top reflection filters using a single photonic crystal slab," *Appl. Phys. Lett.* **84**, 4905–4907 (2004).
30. G. W. Hanson, "Dyadic Green's functions and guided surface waves for a surface conductivity model of graphene," *J. Appl. Phys.* **103**, 064302 (2008).
31. A. Mahigir, T. W. Chang, A. Behnam, G. L. G. Liu, M. R. Gartia, and G. Veronis, "Plasmonic nanohole array for enhancing the SERS signal of a single layer of graphene in water," *Sci. Rep.* **7**, 14044 (2017).
32. D. E. Aspnes and A. A. Studna, "Dielectric functions and optical parameters of Si, Ge, GaP, GaAs, GaSb, InP, InAs, and InSb from 1.5 to 6.0 eV," *Phys. Rev. B* **27**, 985–1009 (1983).
33. J. R. DeVore, "Refractive indices of rutile and sphalerite," *J. Opt. Soc. Am.* **41**, 416–419 (1951).
34. R. C. Weast, M. J. Astle, and W. H. Beyer, *CRC Handbook of Chemistry and Physics* (CRC Press, 1988).
35. S. J. Orfanidis, *Electromagnetic Waves and Antennas* (Rutgers University, 2002).
36. H.-C. Chung, C.-P. Chang, C.-Y. Lin, and M.-F. Lin, "Electronic and optical properties of graphene nanoribbons in external fields," *Phys. Chem. Chem. Phys.* **18**, 7573–7616 (2016).
37. K. Sasaki, K. Kato, Y. Tokura, K. Oguri, and T. Sogawa, "Theory of optical transitions in graphene nanoribbons," *Phys. Rev. B* **84**, 085458 (2011).
38. H. Hsu and L. E. Reichl, "Selection rule for the optical absorption of graphene nanoribbons," *Phys. Rev. B* **76**, 045418 (2007).
39. H. C. Chung, M. H. Lee, C. P. Chang, and M. F. Lin, "Exploration of edge-dependent optical selection rules for graphene nanoribbons," *Opt. Express* **19**, 23350–23363 (2011).